Molecular Crystals and Liquid Crystals Science and Technology. Section A. Molecular Crystals and Liquid Crystals

Publication details, including instructions for authors and subscription information:
http://www.tandfonline.com/loi/gmcl19

Tensor and Complex Representations of Anchoring in Liquid Crystals

S. V. Shiyanovskii [a c], A. Glushchenko [b], Yu. Reznikov [b c], O. D. Lavrentovich [a] & J. L. West [a]

[a] Liquid Crystal Institute, Kent State University, Kent, OH, 44242, USA

[b] Institute of Physics, 46, Prospect Nauki, Kyiv, 03039, Ukraine

[c] Institute for Nuclear Research, 47 Prosp. Nauki, Kyiv, 03039, Ukraine

Version of record first published: 24 Sep 2006

To cite this article: S. V. Shiyanovskii, A. Glushchenko, Yu. Reznikov, O. D. Lavrentovich & J. L. West (2001): Tensor and Complex Representations of Anchoring in Liquid Crystals, Molecular Crystals and Liquid Crystals Science and Technology. Section A. Molecular Crystals and Liquid Crystals, 367:1, 239-250

To link to this article: http://dx.doi.org/10.1080/10587250108028643

Mol. Cryst. and Liq. Cryst., 2001, Vol. 367, pp. 239-250
Reprints available directly from the publisher
Photocopying permitted by license only

Tensor and Complex Representations of Anchoring in Liquid Crystals

S.V. SHIYANOVSKII[ac], A. GLUSHCHENKO[b], YU. REZNIKOV[bc], O.D. LAVRENTOVICH[a] and J.L. WEST[a]

[a]*Liquid Crystal Institute, Kent State University, Kent, OH 44242, USA,* [b]*Institute of Physics, 46, Prospect Nauki, Kyiv, 03039 Ukraine and* [c]*Institute for Nuclear Research, 47 Prosp. Nauki, Kyiv, 03039, Ukraine*

We propose a tensor description of surface anchoring of liquid crystals (LCs). The model allows one to consider both the homogeneous and inhomogeneous parts of LC anchoring and to calculate the cumulative effect of different treatments as a sum of corresponding tensors. For the planar alignment the tensor representation is reduced to the complex azimuthal anchoring coefficient, whose amplitude and phase determine, respectively, the strength of azimuthal anchoring and the azimuthal angle of the easy axis. We predict and experimentally confirm that two consecutive photoalignment treatments with beams of perpendicular polarizations can compensate each other and restore the initial anchoring.

Keywords: liquid crystal; anchoring; tensor representation

INTRODUCTION

Bounding surfaces play a crucial role in the behavior of liquid crystals (LCs) in confined geometries. The surface lifts the degeneracy of the director orientation and sets it along a particular 'easy' direction. Depending on the symmetry of molecular interactions at the interface, the easy direction can be a unique axis or it can be degenerate with respect to rotations around the normal to the boundary.

Until 90s, the only practical technique to align LCs was to set a fixed anchoring direction before the LC cell was assembled, for example, by depositing SiO_x or by buffing a polymer layer. Once assembled, the cells preserved the anchoring characteristics. The situation has been changed by the discovery of photoalignment techniques that allow one to *align* and *realign* the director in a filled cell. Light irradiation could align LC uniformly on an untreated photosensitive substrate or even reorient the director from the easy axis set by a previous treatment, such as polymer buffing. For example, Ichimura[1] demonstrated a light-induced anchoring transition between uniaxial planar (in-plane) and homeotropic (perpendicular to the plane) orientations, while Gibbon et. al.[2-3] and Reznikov et. al.[4-6] used polarized light to reorient the easy axis in the plane of the substrate.

Effective *in situ* photocontrol of LC alignment opens new promising perspectives for recording, processing and storage of optical information[7]. The fundamental aspects are of no lesser importance. The photoalignment technique involves molecular-level changes at the interface, which are often reversible (such as trans-cis isomerisation used in Ichimura's effect[1]). This feature allows one to realign the director *in-situ* and thus to explore how subsequent treatments of the substrate interfere with each other. Furthermore, from a practical standpoint, an ideal photoalignment technique should be applied to a non-treated substrate, which might be amorphous or polycrystalline. Director alignment at such substrate is principally different from that at an isotropic interface (with a fluid or a gas) and is itself an interesting problem. For the isotropic fluid substrate, the surface director orientation is truly degenerate in the plane of the interface. A solid substrate is isotropic only macroscopically, and anisotropic molecular interactions define *local* anchoring axes correlated over distances defined by the particular amorphous or polycrystalline structure of the substrate. We will call such type of anchoring inhomogeneous or random.

The traditional description of the LC anchoring operates with the axis of easy director orientation $\hat{\mathbf{e}}$ and the anchoring energy W that characterizes the work required to deviate the director $\hat{\mathbf{n}}$ from the easy axis. Deviations from the easy axis in the polar and azimuthal planes are characterized by two scalar coefficient W_p and W_a, respectively. This model is not well suited to describe the processes of alignment and re-alignment, when all the relevant quantities such as the easy axis, W_p and W_a change.

In this paper, we propose a tensor phenomenological description of surface anchoring in LCs by presenting the surface energy per unit area as

$$f_s = -\frac{1}{2}\sum_{\alpha,\beta} W_{\alpha\beta}(\mathbf{r})\, n_\alpha\, n_\beta \ , \qquad (1)$$

where $W_{\alpha\beta}(\mathbf{r})$ is the traceless symmetrical local anchoring tensor[8]. It allows us to consider both homogeneous and inhomogeneous parts of anchoring and offers a natural way of handling the problems listed above. We also present an experimental illustration of the proposed approach.

THEORY

Tensor approach.

To derive Eq.(1), we refer to the model of a polymer alignment layer, with the Maier-Saupe pair interaction between LC molecules and polymer fragments. Under the assumption that the polymer alignment does not disturb the surface scalar order parameter S_b, f_s reads:

$$f_s = f_{is}\left((\hat{\mathbf{n}}\cdot\hat{\mathbf{k}})^2\right) - \frac{1}{\sigma}\sum_i\sum_{j\in\sigma} w(\mathbf{r}_i\text{-}\mathbf{r}_j)\mathrm{P}_2(\hat{\mathbf{m}}_i\cdot\hat{\mathbf{l}}_j) \ , \qquad (2)$$

where $\sum_{j\in\sigma}$ is a sum over polymer fragments inside the small area σ, P_2 denotes the second order Legendre polynomial, $\hat{\mathbf{m}}_i$ (or $\hat{\mathbf{l}}_j$) defines orientation of the long axis of the i^{th} LC molecule (or the j^{th} polymer fragment) positioned at $\mathbf{r}_i$ (or $\mathbf{r}_j$) and $w(\mathbf{r}_i\text{-}\mathbf{r}_j)$ is the potential of the anisotropic interaction between the LC molecule and the polymer fragment. f_{is} is the surface energy density on the surface with isotropically distributed polymer fragments, which is an even function of the product of $\hat{\mathbf{n}}$ and the unit surface normal $\hat{\mathbf{k}}$ [9]. Far from the anchoring transition $f_{is} \approx B_0 + B_1(\hat{\mathbf{n}}\cdot\hat{\mathbf{k}})^2$ (B_0 and B_1 are constants) and averaging over orientations of LC molecules one obtains Eq.(1). For a short-range potential $w(\mathbf{r}_i\text{-}\mathbf{r}_j)$, the anchoring tensor $\mathrm{W}_{\alpha\beta}(\mathbf{r})$ is represented as:

$$\mathrm{W}_{\alpha\beta}(\mathbf{r}) = \overline{W}SL_{\alpha\beta}(\mathbf{r}) - 2B_1\left(k_\alpha k_\beta - \tfrac{1}{3}\delta_{\alpha\beta}\right). \qquad (3)$$

Here $\overline{W} = \frac{2}{\sigma}\sum_{j\in\sigma}\sum_{i} w(\mathbf{r}_i\text{-}\mathbf{r}_j)$, and $L_{\alpha\beta}(\mathbf{r}) = < l_j^{\alpha}(\mathbf{r}) l_j^{\beta}(\mathbf{r}) > -\frac{1}{3}\delta_{\alpha\beta}$ is the local tensor order parameter of the polymer fragments. Minimum of the surface energy (1) can be easily found in the frame $\{\hat{\mathbf{e}}_j\}$ (j=1,2,3), where $W_{\alpha\beta}(\mathbf{r})$ is diagonal with eigenvalues $W_1 > W_2, W_3$. In the frame $\{\hat{\mathbf{e}}_j\}$, which is orthogonal due to the symmetry of $W_{\alpha\beta}(\mathbf{r}) = W_{\beta\alpha}(\mathbf{r})$, Eq.(1) reads :

$$f_s = -\frac{W_1}{2} + \frac{W_1 - W_2}{2} n_2^2 + \frac{W_1 - W_3}{2} n_3^2, \tag{4}$$

where n_j are the director components in this frame. The second and the third terms in (4) are non-negative, so that the axis $\hat{\mathbf{e}}_1$, which corresponds to the maximum eigenvalue W_1, is exactly the easy axis, while the quantities $(W_1 - W_2)$ and $(W_1 - W_3)$ determine the traditional azimuthal and polar anchoring coefficients.

Comparison of Eq.(1) and Eq.(4) shows the difference between the tensor and the traditional approaches. The traditional description is equivalent to the tensor one in the eigen frame $\{\hat{\mathbf{e}}_j\}$. This frame rotates from point to point and during a treatment, making the description cumbersome. The tensor description has the covariant form and thus describes random anchoring and consecutive treatments in any reference frame.

To analyze the anchoring properties of a substrate one has to distinguish the local anchoring tensor $W_{\alpha\beta}(\mathbf{r})$ and its macroscopic average over the whole surface $\langle W_{\alpha\beta}(\mathbf{r})\rangle_r$. A non-treated substrate has macroscopic azimuthal symmetry. Therefore, the average polymer tensor order parameter $\langle L^{in}_{\alpha\beta}(\mathbf{r})\rangle_r$ for a non-treated inhomogeneous substrate should be diagonal in the $0xyz$ frame ($0z$ is normal to the substrate) with diagonal elements $\langle L^{in}_{xx}(\mathbf{r})\rangle_r = \langle L^{in}_{yy}(\mathbf{r})\rangle_r = L_{\parallel}$ and $\langle L^{in}_{zz}(\mathbf{r})\rangle_r = L_{\perp}$. According to Eq.(3), the average anchoring tensor $\langle W^{in}_{\alpha\beta}(\mathbf{r})\rangle_r$ should have the same form $\langle W^{in}_{xx}(\mathbf{r})\rangle_r = \langle W^{in}_{yy}(\mathbf{r})\rangle_r = W_{\parallel}$ and $\langle W^{in}_{zz}(\mathbf{r})\rangle_r = W_{\perp}$. Since the two diagonal elements are equal, orientation of the easy axis is degenerate (the only exception is strictly normal orientation). Therefore, even small deviation of $W^{in}_{\alpha\beta}(\mathbf{r})$ from $\langle W^{in}_{\alpha\beta}(\mathbf{r})\rangle_r$, caused by local

inhomogeneity in orientation of aligning fragments, lifts the degeneracy and sets a unique orientation of the local easy axis.

The photoalignment on polymer surface can be caused by different mechanisms. Some of these mechanisms might be reversible (cis-trans isomerization) and some of them might be irreversible (formation of permanent covelent bonds). All mechanisms lead to additional orientational order of aligning fragments. If the initial local variations of the polymer order are small, $\left|L^{in}_{\alpha\beta}(\mathbf{r}) - \langle L^{in}_{\alpha\beta}(\mathbf{r})\rangle_r\right| << 1$, the additional order $L^{k}_{\alpha\beta}(\mathbf{r})$, caused by the k^{th} uniform treatment, does not depend on these variations and is also uniform: $L^{k}_{\alpha\beta}(\mathbf{r}) = \langle L^{k}_{\alpha\beta}(\mathbf{r})\rangle_r = L^{k}_{\alpha\beta}$. Thus, the 'weak' treatments, which affect only small fraction of polymer fragments, lead to the final anchoring tensor $W(\mathbf{r})$ that is simply a sum of the random initial anchoring $W^{in}(\mathbf{r})$ and the contributions $W^{(k)}$ of different treatments:

$$W(\mathbf{r}) = W^{in}(\mathbf{r}) + \sum_k W^{(k)} , \qquad (5)$$

where $W^{(k)}$ is diagonal in the frame which corresponds to induced easy axis $\hat{\mathbf{e}}^{(k)}$ .The effect of 'strong' treatments, which reorient a substantial fraction of the polymer fragments, can also be expressed with Eq.(5), but in this case $W^{(k)}$ are nonlinear functions of the irradiation times τ_k and the sequence of different treatments is crucial (the treatments are non-commutative).

One has to clearly understand the difference between the of tensor presentation of anchoring (1) and anchoring potential for systems with spatially inhomogeneous tensor order parameter $Q_{\alpha\beta}(\mathbf{r})$ [10,11], which is the generalization of the Rapini-Papoular potential[12]:

$$f_s = \frac{1}{2} A \mathrm{Tr}\left[\left(Q^b_{\alpha\beta} - Q^0_{\alpha\beta}\right)^2\right] \qquad (6)$$

where A is the scalar anchoring strength, $Q^b_{\alpha\beta}$ is the surface value of the tensor order parameter, $Q^0_{\alpha\beta} = \frac{3}{2} S_0 (n_{0\alpha} n_{0\beta} - \frac{1}{3}\delta_{\alpha\beta})$ is the preferred surface value of the tensor order parameter. For the uniaxial phase $Q^b_{\alpha\beta} = \frac{3}{2} S_b (n_\alpha n_\beta - \frac{1}{3}\delta_{\alpha\beta})$ and the potential (6) simplifies to the form:

$$f_s = \frac{1}{2} A \frac{3}{2} \left\{ S_b^2 + S_0^2 - S_b S_0 \left[3(\mathbf{n} \cdot \mathbf{n}_0)^2 - 1 \right] \right\} \tag{7}$$

which is the axially symmetric form of Rapini-Papoular potential (the axis of symmetry being the easy axis $\mathbf{n}_0$) with a coefficient, that depends on the surface value of orientational order. Thus, although Eqs. (6) and (7) deal with the tensor order parameter, the anchoring in an uniaxial phase is a *scalar* quantity.

Complex representation for planar anchoring.

Substantial simplification can be achieved for the tangential (in-plane) alignment that corresponds to the conditions $W_{yz} = W_{xz} = 0$. In this case, it is possible to specify the director on a complex plane: $\tilde{n} = n_x + i n_y = \cos\theta e^{i\varphi}$, where θ is a polar angle and φ is an azimuthal angle of the director. In this representation, the surface energy (1) takes a form:

$$\begin{aligned} f_s &= f_{s0} + \frac{1}{8}\left(\tilde{W}_a^* \tilde{n}\tilde{n} + \tilde{W}_a \tilde{n}^* \tilde{n}^* \right) + \frac{3}{4} W_{zz} \left(1 - \tilde{n}\tilde{n}^* \right) \\ &= f'_{s0} + \frac{1}{2} W_a \cos^2\theta \sin^2(\varphi - \psi) + \frac{1}{2} W_p \sin^2\theta \end{aligned} , \tag{8}$$

where $\tilde{W}_a = W_{xx} - W_{yy} + i W_{xy} = W_a e^{i2\psi}$ is the complex azimuthal anchoring coefficient and $W_p = \frac{1}{2}(W_a - 3W_{zz})$.

The complex representation has the following advantages:

(1) W_p, W_a and ψ in Eq.(8) and in the definition $\tilde{W}_a = W_a e^{i2\psi}$ are simply the traditional anchoring coefficients and the azimuthal angle of easy axis, respectively.

(2) $\tilde{W}_a$ is the linear combination of tensor components, thus the complex representation preserves the additivity of different treatments:

$$\tilde{W}_a(\mathbf{r}) = \tilde{W}_a^{in}(\mathbf{r}) + \sum_k \tilde{W}_a^{(k)} \tag{9}$$

(3) Any treatment can be presented in a compact form $\tilde{W}_a^{(k)} = W_a^{(k)} \exp(2i\psi_k)$, where the phase describes the orientation ψ_k of the induced easy axis and the amplitude W_a^k corresponds to the strength of the treatment. One can visualize different treatments graphically presenting $\tilde{W}_a^{(k)}$ by vectors in the complex plane, Fig.1,2.

We illustrate the complex representation by the following examples. A substrate with a uniform in-plane easy axis is irradiated with polarized light that produces a different easy axis. According to Eq.(9) the resulting complex anchoring $\tilde{W}_a$ is the sum of the initial anchoring $\tilde{W}_a^{(1)} = W_a^{(1)} \exp(2i\psi_1)$ and light-induced anchoring $\tilde{W}_a^{(2)} = W_a^{(2)} \exp(2i\psi_2)$ (Fig.1). The amplitude $W_a^{(2)}$ is controlled by exposure. When the initial and the light-favored easy axes are not perpendicular, the increase of $W_a^{(2)}$ leads to continuous rotation of the easy axis $\hat{\mathbf{e}}$ from ψ_1 to ψ_2 or to $\psi_2 + \pi$, whichever is closer to ψ_1 (dashed curve, Fig.1). When the two are perpendicular, $\psi_2 = \psi_1 + \pi/2$, the dashed curve collapses into the right angle and there is no continuous reorientation. In this case, when the treatment is weak, $W_a^{(2)} < W_a^{(1)}$, the resulting easy axis does not move, but the strength of the anchoring decreases, $W_a \to 0$. When $W_a^{(2)} > W_a^{(1)}$, the easy axis abruptly realigns from ψ_1 to $\psi_2 = \psi_1 + \pi/2$.). Both the smooth rotation[13,14] and the threshold realignment[15] have already been observed.

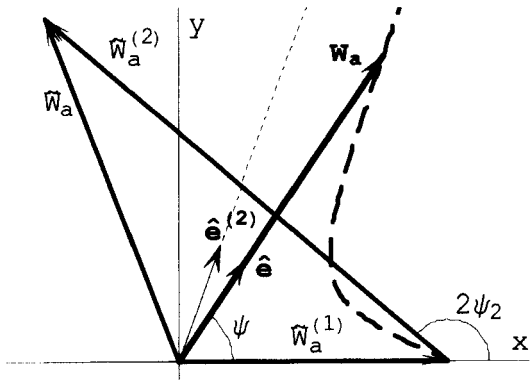

FIGURE. 1. Graphic representation of the cumulative effect of two homogeneous treatments with different induced easy axes: $\hat{\mathbf{e}}^{(1)} \| 0x$ and $\hat{\mathbf{e}}^{(2)}$ making the angle ψ_2 with $0x$ axis; dashed curve shows the trajectory of the vector $\mathbf{W}_a = W_a \hat{\mathbf{e}}$ when $W_a^{(2)}$ increases.

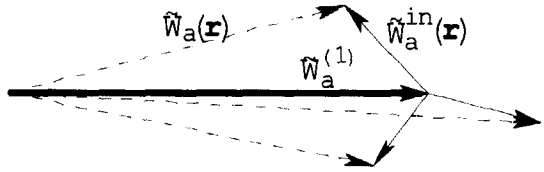

FIGURE. 2. Graphic representation of the effect of the unidirectional homogeneous treatment $\tilde{W}_a^{(1)}$ (thick arrow) at different points of an inhomogeneous substrate with local anchorings $\tilde{W}_a^{in}(\mathbf{r})$ (thin arrows); $\tilde{W}_a(\mathbf{r})$ (dashed arrows) are the resulting anchorings at the same points of the surface.

In a similar way, Eq.(9) describes the effect when an inhomogeneous substrate is subjected to a uniform alignment treatment $\tilde{W}_a^{(1)}$ (Fig.2). This treatment 'hides' the random anchoring rather than destroys it; the resulting $\tilde{W}_a(\mathbf{r})$ is the vector sum of $\tilde{W}_a^{(1)}$ and the local anchoring $\tilde{W}_a^{in}(\mathbf{r})$. This feature predicts an interesting and counterintuitive effect: the original random anchoring modified by the unidirectional treatment $W_a^{(1)}$ can be restored by a subsequent treatment of the same amplitude $W_a^{(2)} = W_a^{(1)}$ but of the orthogonal direction $\psi_2 = \psi_1 + \pi/2$, i.e., $\tilde{W}_a^{(2)} = -\tilde{W}_a^{(1)}$. The validity of the tensor and complex description and in particular, the compensating effect of two treatments, $\tilde{W}_a^{(2)} = -\tilde{W}_a^{(1)}$, is demonstrated experimentally below.

EXPERIMENT

We study nematic LC 5CB (Merck) and a photoaligning polymer para-fluoro-cinnamoyl cellulose (FCCN), which aligns 5CB tangentially. 5CB is placed between the reference and the FCCN substrates. The reference substrate is a rubbed polyimide layer that produces strong planar anchoring along the rubbing direction $\hat{\mathbf{e}}_{rub}$. The cell thickness is large, L = 55 μm, to reduce the elastic torque $\sim K_{22}/L$.

Inhomogeneous anchoring at non-treated FCCN substrate.
The cell was filled with 5CB in the isotropic state (T=100°C). The FCCN substrate was put in contact with a cooled surface to create a temperature

gradient across the cell. The nematic phase nucleated at the FCCN surface first, and then propagated towards the reference plate. In this way, alignment of LC at FCCN was determined mainly by the anchoring properties of the FCCN surface. The alignment is inhomogeneous with characteristic size of domains $d \sim 100$ μm, Fig.3a. The reference rubbed surface faced the polarizer of the microscope, with $\hat{\mathbf{e}}_{rub}$ being parallel to the polarizer. The polarization of the transmitted light is determined by the local director orientation on the FCCN substrate ("Mauguin regime"). The total intensity of the transmitted light did not depend on the orientation of the analyzer within an error of 10 %. Thus the local azimuthal anchoring W_a^{FCCN} at FCCN surface is random and strong enough to withstand the orienting action of the reference rubbed substrate, $W_a^{FCCN} >> K_{22}/L$, and the increase of elastic energy, caused by inhomogeneities $W_a^{FCCN} >> K_{33}/d$ [16,17].

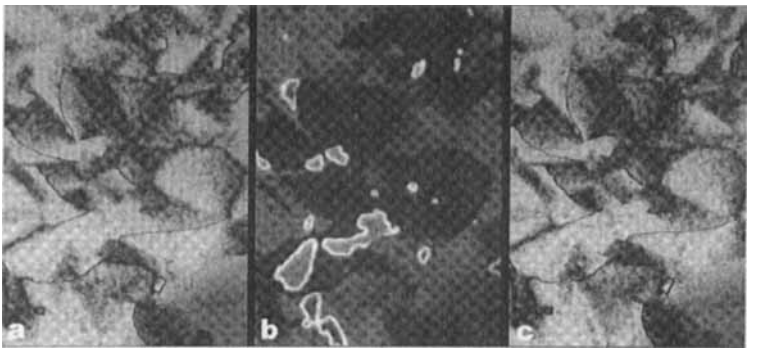

FIGURE 3. The textures of the same spot (about 250 μm wide) before irradiation (a), after the first irradiation with $\hat{\mathbf{e}}_{uv}^{(1)} \perp \hat{\mathbf{e}}_{rub}$, $\tau_1 = 15$ s (b), and after the second irradiation with $\hat{\mathbf{e}}_{uv}^{(2)} \parallel \hat{\mathbf{e}}_{rub}$, $\tau_2 = 45$ s (c). Parallel polarizers.

The random alignment pattern was stable; we removed the LC from the cell followed by the cell was filled again (Fig.4) and the new pattern did not differed from the initial one. It means that the pattern exhibits a local anisotropy of the FCCN surface rather than uncontrollable factors in filling and cooling of the cell.

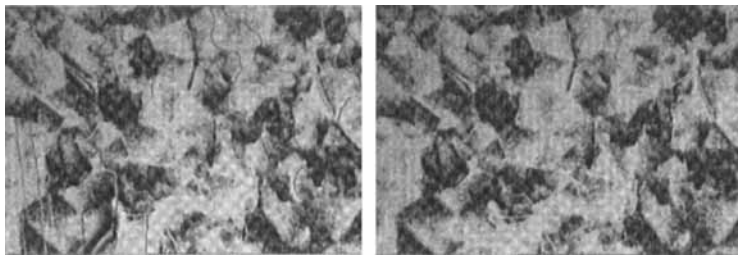

FIGURE.4. The textures of the same spot after the first cell filling (a) and after the secondary filling (b).

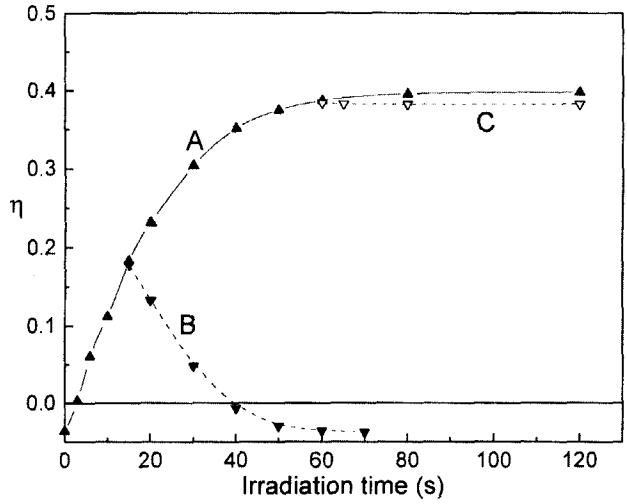

FIGURE 5. The transmittance anisotropy η vs. irradiation time. Curve A corresponds to the first irradiation with $\hat{\mathbf{e}}_{uv}^{(1)} \perp \hat{\mathbf{e}}_{rub}$. Curves B and C result from the second irradiation with $\hat{\mathbf{e}}_{uv}^{(2)} \| \hat{\mathbf{e}}_{rub}$ that follows the first irradiation of duration $\tau_1 = 15$ s and $\tau_1 = 60$ s, respectively.

Alignment by polarized light.
The cell described above was exposed to polarized UV light (500W Hg lamp, intensity 5 mW/cm^2) that is absorbed effectively by FCCN. The induced alignment direction $\hat{\mathbf{e}}_{uv}$ is perpendicular to the polarization of the incident light. Irradiation reorients $\hat{\mathbf{n}}$ towards $\hat{\mathbf{e}}_{uv}$ and produces macroscopic optical anisotropy of the cell. To quantify the anisotropy we use the parameter $\eta = (I_{\parallel} - I_{\perp})/(I_{\parallel} + I_{\perp})$, where $I_{\parallel}$ and $I_{\perp}$ are the intensities of transmitted light measured with analyzer parallel and perpendicular to $\hat{\mathbf{e}}_{uv}$, respectively. The dependence of η on the exposure time τ (Fig.5, curve A) corresponds to the scenario depicted in Fig.2 and reveals the non-linear effect with saturation.

Compensating effect of two orthogonal irradiations.
To demonstrate the recovery of the initial inhomogeneous anchoring, the cell with non-treated substrate (Fig.3a) was subjected to two subsequent UV orthogonal treatments. The first treatment with $\hat{\mathbf{e}}^{(1)}_{uv} \perp \hat{\mathbf{e}}_{rub}$ during τ_1 = 15 s induced a 90^0 twist structure in the cell (Fig.3b). The bright lines in Fig.2b correspond to domain walls that separate regions with opposite rotations. The second treatment with $\hat{\mathbf{e}}^{(2)}_{uv} \perp \hat{\mathbf{e}}^{(1)}_{uv}$ (Fig.5, curve B) exhibits the mirror behavior in comparison with curve A with respect to the value of η between the irradiations. The texture obtained after τ_2 = 45 s when η returns to its initial value $\eta(\tau = 0)$, Fig.3c, is essentially identical to the initial texture, Fig.3a, i.e. the second exposure recovers the initial pattern $\hat{\mathbf{n}}(\mathbf{r})$ in details. If $\tau_1 > 15$ s the recovery of $\eta(\tau = 0)$ is not achievable, although $\eta(\tau)$ clearly preserves the mirror behavior (Fig.5, curve C). The recovery of the initial texture in the saturation range for the second treatment confirms the validity of Eq.(5) and Eq.(9) even for strong treatments.

Acknowledgments

The authors are grateful to Igor Gerus for the synthesis of FCCN. The work was supported by the NSF ALCOM Grant No DMR89-20147, by the CRDF Joint Grant No 7283/6548 and by the Fund of the Academy of Sciences of Ukraine, Grant No B29/13.

References

[1] K. Ichimura, in *Photochemical Processes in Organized Molecular Systems*, edited by K. Honda (Elsevier, Amsterdam, 1991), p. 343.
[2] W. Gibbon, P. Shannon, S.T. Sun, B. Swetlin. *Nature*, **351**, 6321 (1991).
[3] W. Gibbons, T. Kosa, P. Pulffy-Muhoray, P. Shannon, S.T. Sun. *Nature*, **377**, 43 (1995).
[4] T. Marusii and Yu. Reznikov. *Mol. Mater.* **3**, 1614 (1993).
[5] A. Dyadyusha, Yu. Reznikov, V. Reshetnyak, *Mol. Mater.* **5**, 183 (1995).

[6] D. Voloshchenko, A. Khizhnyak, Yu. Reznikov, V. Reshetnyak. *Jap. Journ. Appl. Phys.* **34** 566 (1995).
[7] See, e.g., F. Simoni and O. Francescangeli, *J. Phys.: Condens. Matter* **11**, R439 (1999).
[8] S.V. Shiyanovskii, A. Glushchenko, Yu. Reznikov, O.D. Lavrentovich, and J.L. West. *Phys. Rev. E*, **62**, (2000) (in press).
[9] T.J. Sluckin and A. Poniewierski, in *Fluid Interfacial Phenomena*, edited by C.A. Croxton (Wiley, New York, 1985), p. 215.
[10] M. Nobili and G. Durand. *Phys. Rev. A*, **46**, R6174 (1992).
[11] A. Sarlah and S. Zumer. *Phys. Rev. E*, **60**, 1821 (1999).
[12] A. Rapini and M. Papoular, *J. Phys. (Paris) Colloq.* **30**, C-4 (1969).
[13] J. Chen, D.L. Johnson, P.J. Bos, X. Wang, and J.L. West. *Phys. Rev. E*, **54**, 1599 (1996).
[14] J.H. Kim, S. Kumar, Sin-Doo Lee. *Phys. Rev. E*, **57**, 5644 (1998).
[15] A.G. Dyadyusha, T. Ya. Marusii, V. Yu. Reshetnyak, Yu. A. Reznikov, A.I. Khizhnyak. *JETP Lett.*, **56**, 17 (1992).
[16] O.D. Lavrentovich and P. Palffy-Muhoray, Liq. *Cryst. Today* **5** #2, 5 (1995).
[17] J.-B. Fournier and P. Galatola, *Phys. Rev. Lett.* **82**, 4859 (1999).